

Cytokinin-promoted secondary growth and nutrient storage in the perennial stem zone of *Arabis alpina*

Anna Sergeeva^{1,2}, Hongjiu Liu¹, Hans-Jörg Mai¹, Tabea Mettler-Altmann^{2,3}, Christiane Kiefer⁴, George Coupland^{2,4} and Petra Bauer^{1,2,*} 

¹Institute of Botany, Heinrich Heine University, Düsseldorf D-40225, Germany,

²Cluster of Excellence on Plant Science (CEPLAS), Heinrich Heine University, Düsseldorf, Germany,

³Institute of Plant Biochemistry, Heinrich Heine University, Düsseldorf D-40225, Germany, and

⁴Department of Plant Developmental Biology, Max Planck Institute for Plant Breeding Research, Cologne D-50829, Germany

Received 1 June 2020; accepted 30 November 2020.

*For correspondence (e-mail Petra.Bauer@hhu.de).

SUMMARY

Perennial plants maintain their lifespan through several growth seasons. *Arabis alpina* serves as a model Brassicaceae species to study perennial traits. Lateral stems of *A. alpina* have a proximal vegetative zone with a dormant bud zone and a distal senescing seed-producing inflorescence zone. We addressed how this zonation is distinguished at the anatomical level, whether it is related to nutrient storage and which signals affect the zonation. We found that the vegetative zone exhibits secondary growth, which we termed the perennial growth zone (PZ). High-molecular-weight carbon compounds accumulate there in cambium and cambium derivatives. Neither vernalization nor flowering were requirements for secondary growth and the sequestration of storage compounds. The inflorescence zone with only primary growth, termed the annual growth zone (AZ), or roots exhibited different storage characteristics. Following cytokinin application cambium activity was enhanced and secondary phloem parenchyma was formed in the PZ and also in the AZ. In transcriptome analysis, cytokinin-related genes represented enriched gene ontology terms and were expressed at a higher level in the PZ than in the AZ. Thus, *A. alpina* primarily uses the vegetative PZ for nutrient storage, coupled to cytokinin-promoted secondary growth. This finding lays a foundation for future studies addressing signals for perennial growth.

Keywords: *Arabis alpina*, perennial, cytokinin, cambium, secondary growth, lipid body, starch.

INTRODUCTION

Perennial plants sustain their lifespan through several growth seasons and many of these plants are polycarpic and reproduce multiple times (Bergonzi and Albani, 2011). This allows the plants to maintain space in their environment in order to exploit and defend light and soil resources and survive harsh conditions. In contrast, annual plants are usually monocarpic and reproduce only once before they die (Thomas, 2013), a lifestyle of advantage in lowland dry habitats with animal foraging and agriculture that favors juvenile survival.

Vegetative above-ground shoots of perennial plants may grow in diameter over the years. This production of new tissues in the lateral dimension is termed secondary growth and is initiated by two secondary meristems. The fascicular and interfascicular cambium produces new vasculature in the form of secondary xylem and secondary phloem, and corresponding parenchyma, leading to the

formation of wood and bast. The cork cambium or phellogen produces outward cork and inward phelloderm to generate new protective outer layers, the periderm, with increasing stem diameter. A diverse set of phytohormones and signals influences cambial activity in stems (Fischer *et al.*, 2019). Hormonal profiling across the *Populus trichocarpa* stem identified a specific but interconnected distribution of hormones (Immanen *et al.*, 2016). Cytokinins peaked in the developing phloem tissue, whereas auxin had its maximum in the dividing cambial cells and developing xylem tissue was marked by bioactive gibberellin (Immanen *et al.*, 2016). Cytokinins are key regulators of cambium initiation, and cambial activity is affected in cytokinin biosynthetic mutants and by cytokinin supply (Matsumoto-Kitano *et al.*, 2008; Nieminen *et al.*, 2008). Cambial auxin concentration is relevant for the activity and maintenance of cambium (Immanen *et al.*, 2016), for example through homeobox transcription factors regulating auxin-

dependent cambium proliferation (Suer *et al.*, 2011; Kucukoglu *et al.*, 2017). Gibberellins act in the xylem region promoting xylem cell differentiation and lignification (Denis *et al.*, 2017). Secondary growth is coupled with nutrient allocation. In *Populus*, carbon storage, in the form of triacylglycerols (TAGs), galactose and raffinose, is present in the stem bark and wood tissues (Sauter and van Cleve, 1994; Sauter and Wellenkamp, 1998; Watanabe *et al.*, 2018). Nutrient deposition in storage organs is also affected by plant hormones, and cytokinins may play a dual role in some perennials to direct secondary growth and nutrient storage therein (Hartmann *et al.*, 2011; Eviatar-Ribak *et al.*, 2013).

The perennial life strategy is usually regarded to be ancestral (Hu *et al.*, 2003; Grillo *et al.*, 2009), which is also true for the tribe Arabideae within the Brassicaceae. Interestingly, annuality has evolved multiple times in this tribe independently from a perennial background in different lineages (Karl and Koch, 2013). This suggests that this complex lifestyle decision may be determined by a limited set of regulatory events. Phylogenetic reconstruction has shown that perennial *Arabis alpina* and annual *Arabis montbretiana* are sister species. Hence, these two taxa have been established as a model system to study the perennial–annual transition (Kiefer *et al.*, 2017; Heidel *et al.*, 2016).

Arabis alpina Pajares (Paj), an accession from Spain, was used to characterize the perennial life cycle of the species. These plants have above-ground vegetative perennial parts and stems as well as reproductive parts that senesce and die during the growth season (Wang *et al.*, 2009). A characteristic of perennial vegetative stems is the transition from juvenile to adult phase, which results in flowering (Bergonzi and Albani, 2011; Hyun *et al.*, 2017). Competence to flower in perennial *A. alpina*, as in annual *Arabidopsis thaliana*, can be conferred by the ecologically relevant adaptive trait of vernalization during a cold winter period, which suppresses flowering until the action of repressors is released (Kim *et al.*, 2009; Wang *et al.*, 2009). The positions of individual flowers, dormant buds, and non-flowering and flowering lateral branches vary along the stems of *A. alpina*. From bottom to top, three types of vegetative (V1, V2 and V3) and two inflorescence (I1 and I2) subzones are distinguished, established during and after vernalization (Lazaro *et al.*, 2018). V1 has full lateral branches resembling the main shoot axis in terms of the zonation pattern. V2 has dormant axillary buds, and the short V3 subzone has axillary vegetative branches. I1 has lateral branches forming inflorescences, whereas I2 is an inflorescence and forms individual flowers (Lazaro *et al.*, 2018). The signals and genetic networks triggering the differentiation of V and I zones are not fully understood. *Arabis alpina* PERPETUAL FLOWERING 1 (*PEP1*), similar to its ortholog in *Arabidopsis*, *FLOWERING LOCUS C* (*FLC*), is a

regulator of flowering in response to vernalization and acts as floral repressor (Wang *et al.*, 2009). The *pep1-1* mutant, a derivative of the wild-type accession Paj, shows constant reproduction. Despite lower longevity and the absence of the subzonation of the vegetative stem zone, *pep1-1* plants show perennial growth characteristics and have the ability to continuously form new lateral branches until the end of the growth season (Wang *et al.*, 2009; Hughes *et al.*, 2019). Thus, flowering control pathways are regulated by age control systems to maintain the perennial lifestyle (Hyun *et al.*, 2019). Besides vernalization, auxin signals are also involved (Vayssières *et al.*, 2020).

The regulation of nutrient allocation is fundamental for the perennial life cycle to re-initiate growth. In this study, we provide evidence that the proximal vegetative stem zone is characterized by secondary growth where nutrient storage takes place (termed here the perennial zone, PZ), irrespective of flowering control by *PEP1*. In contrast, the distal reproductive zone has primary growth (termed here the annual zone, AZ). We furthermore show that cytokinin is effective in initiating secondary growth and we propose a heterochronic model for the PZ–AZ transition.

RESULTS

Lateral stems of *A. alpina* plants have a perennial secondary growth zone and an annual primary growth zone

To investigate nutrient storage in *A. alpina* stems, we first inspected the anatomy of stem internode cross sections. As nutrient storage might be coupled with signals for vernalization, besides vernalization-dependent wild-type Pajares (Paj) we also included its mutant derivative *perpetual flowering 1-1* (*pep1-1*), which flowers independently of vernalization. We performed comparisons of perennial lines with the annual sister species *A. montbretiana* that also does not require vernalization. We focused on internodes of the lateral branches, formed in the V1 subzone of the main axis at the lower first to fifth nodes. Subzonation into three V zones (V1, V2 and V3) is present in Paj, but is absent in *pep1-1*. Instead, *pep1-1* has a single V zone, V1, and all axillary buds develop into flowering branches (Wang *et al.*, 2009; Vayssières *et al.*, 2020). Thus, by investigating lateral branches from V1 we were able to study the role of *PEP1* in stem development and nutrient allocation.

The anatomy of these lateral branches changed from the vegetative (V) to the inflorescence (I) zones. Paj V internodes displayed secondary growth, visible as novel tissues formed by cambium and cork cambium activity. As advanced secondary growth is a perennial trait, we termed this zone the ‘perennial zone’ (PZ; Figure 1). The I zone internodes had only primary growth characteristics in Paj and, accordingly, we termed this zone the ‘annual zone’ (AZ; Figure 1). *pep1-1* showed a PZ and an AZ as Paj,

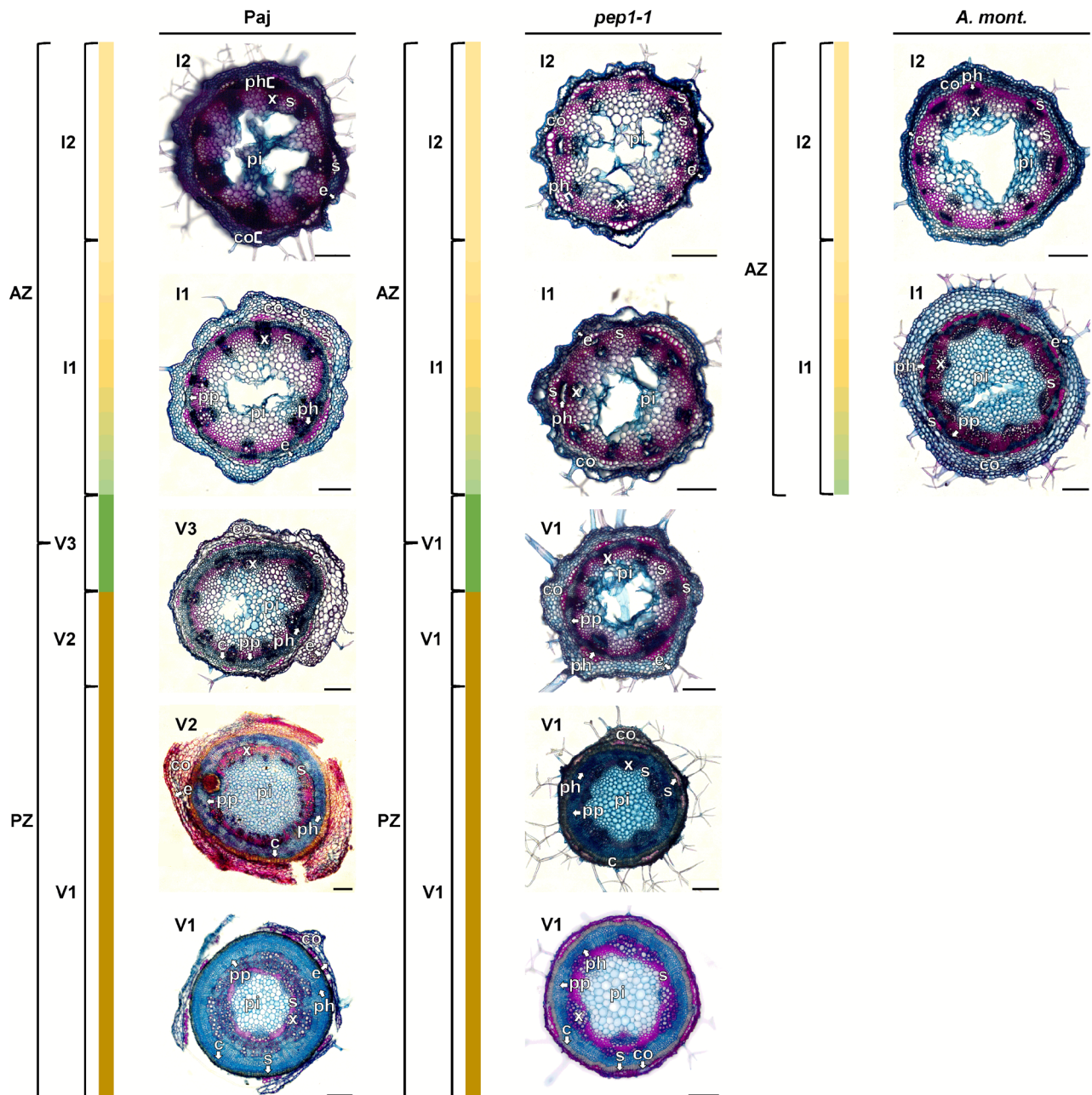


Figure 1. Overview of lateral stem internode anatomy of perennial and annual *Arabis* plants: 100- μ m cross sections of lateral stems formed at the lower nodes of main stems from perennial *Arabis alpina* Pajares (Paj, wild type), its *perpetual flowering 1-1* (*pep1-1*) mutant derivative and annual *Arabis montbretiana* (*A. mont.*). Lateral branches are shown in Figure 2b, where red triangles indicate the positions of the cross sections. A perennial zone (PZ) with secondary growth characteristics is found at the proximal side of lateral branches, corresponding to the vegetative zone (V1 and V2, described for main stems in Lazaro *et al.*, 2018), whereas an annual zone (AZ) with primary growth overlaps with the inflorescence zone (I1 and I2, described in main stems in Lazaro *et al.*, 2018). PZ and AZ are separated by a transition zone (V3, described for main stems in Lazaro *et al.*, 2018). Anatomy investigated following FCA staining: in blue, staining of non-lignified cell walls (parenchyma, phloem and meristematic cells); in red, staining of lignified cell walls; and in greenish color, staining of suberized cell walls (xylem, sclerenchyma and cork). Abbreviations: c, cork; co, cortex; e, epidermis; ph, phloem, including primary phloem, secondary phloem and phloem parenchyma; pi, pith; pp, secondary phloem parenchyma; s, sclerenchyma; x, xylem, including primary xylem, secondary xylem and xylem parenchyma. Arrows point to respective tissues. Scale bars: 200 μ m.

whereas *A. montbretiana* lateral stems displayed the AZ pattern (Figure 1).

Next, we inspected lateral stem anatomy more closely at specific growth stages during the development of the PZ

and the AZ, namely at stage I (after 8 weeks, before vernalization), at stages II and III (after 20 and 35 weeks, including vernalization) and at stage II' (after 20 weeks, without vernalization) (Figure 2; for detailed descriptions of plant

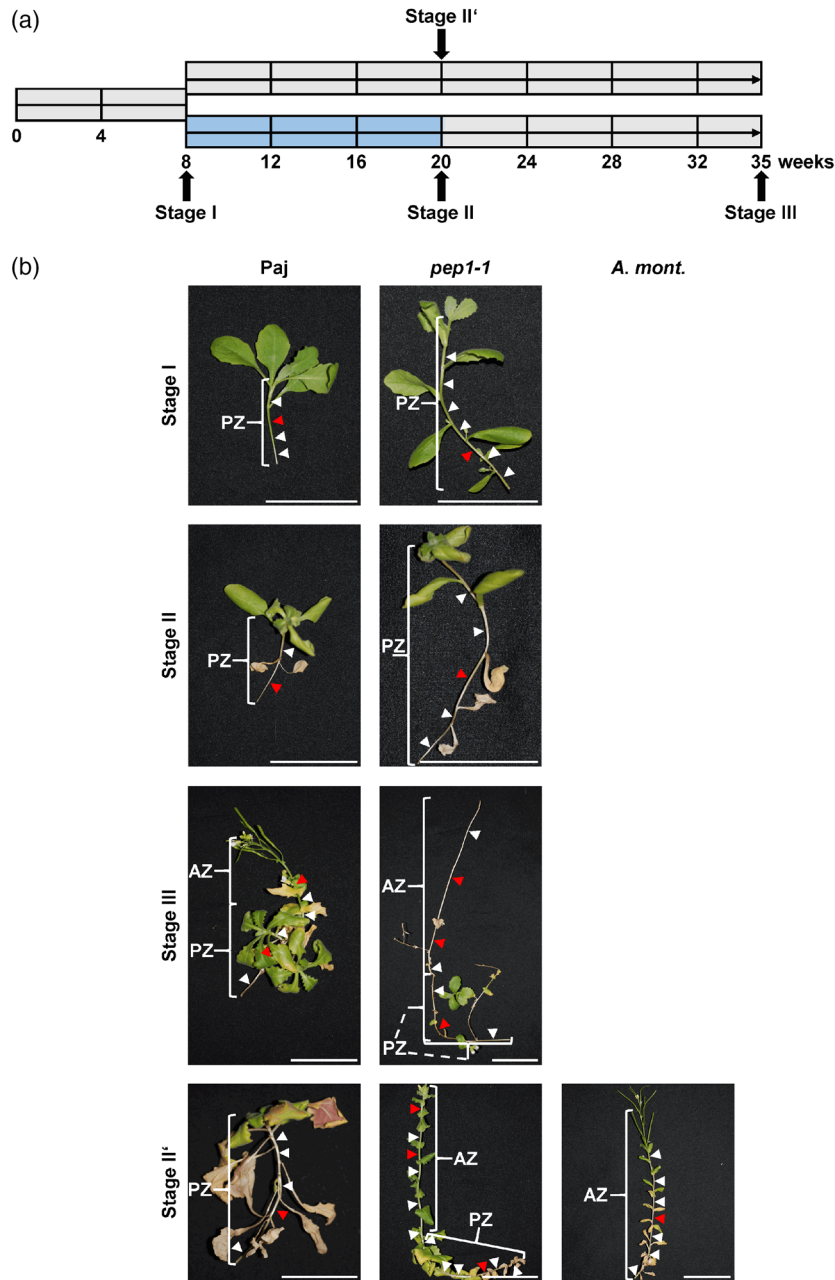


Figure 2. Plant growth and morphology. (a) Plant growth scheme and harvesting stages. Time scale of plant growth: gray, long-day conditions at 20°C; blue, short-day conditions at 4°C (vernalization); harvesting stages I, II and III, or alternatively II'. (b) Lateral stem morphology at different growth stages. Representative photos of lateral stems from lower nodes of the main axis at stages I, II, III and II'; perennial *Arabis alpina* Pajares (Paj, wild type), its *perpetual flowering 1-1* (*pep1-1*) mutant derivative and annual *Arabis montbretiana* (*A. mont.*); for whole-plant morphology, see Figure S2. Red triangles indicate the positions of the cross sections in Figure 3, similar to those shown in Figure 1; white triangles, other regions examined by microscopy. Scale bars: 5 cm.

growth, see Figure S2). At stages I and II, lateral branches were vegetative in character (Figure 2b) and all elongated internodes corresponded to the PZ, with secondary growth beginning to take place, similar to Paj and *pep1-1* (PZ in Figure 3a,b). At stage I (Figure 3a), the epidermis and the cortex were separated from the central pith by a ring of vascular bundles. The cambium was narrow, surrounded

by a few layers of secondary phloem. We noted a ring of cork cambium below the sclerenchyma cap in vascular bundles and below the outer cortex in the interfascicular region. Cork cells had already formed in some regions (note that this tissue became more evident at later stages). At stage II (Figure 3b), cork formation underneath the outer cortex had progressed to a multi-cell-layer-thick ring in the

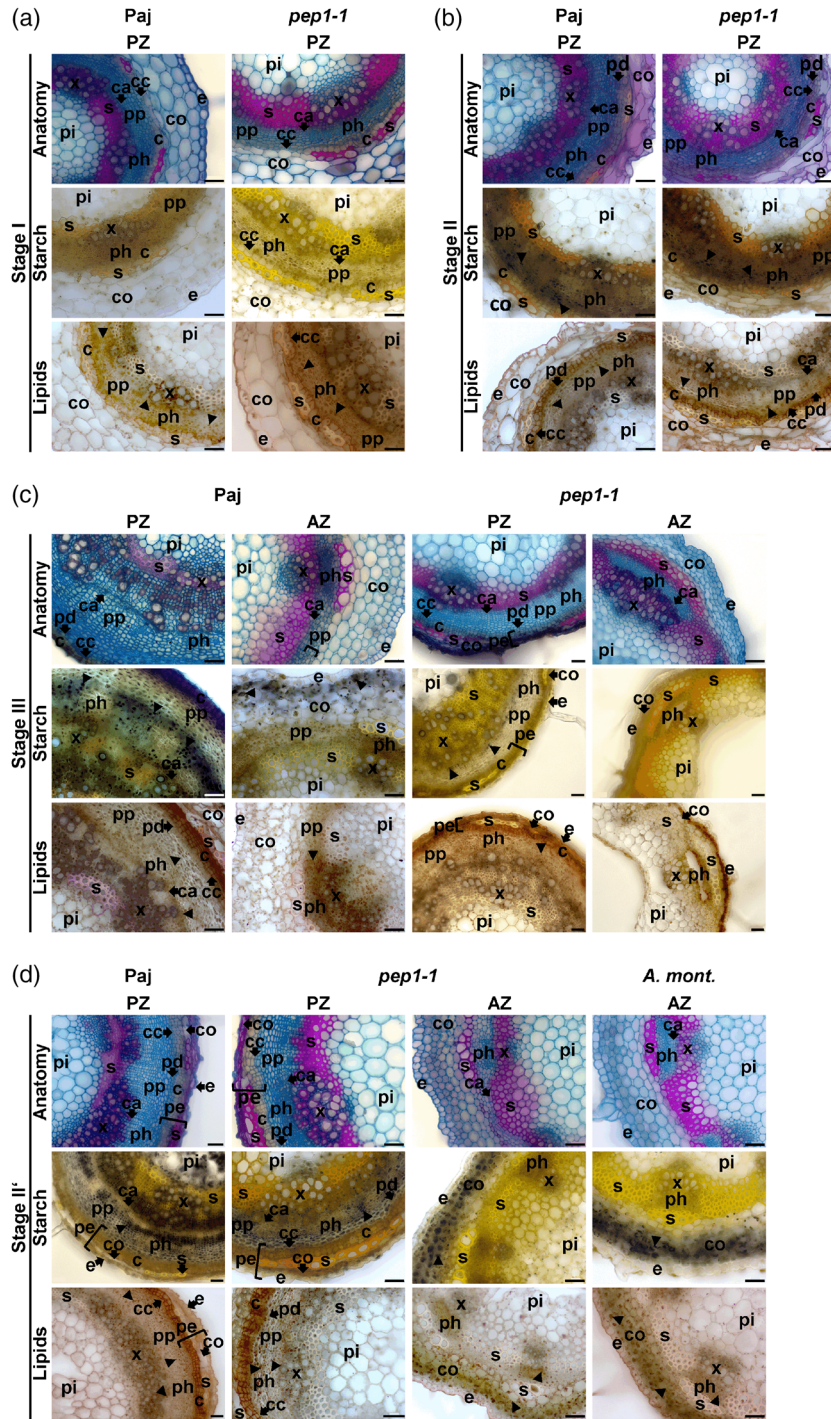


Figure 3. Anatomy, starch and lipid body staining of lateral stem internodes. Representative lateral stem internode cross sections at: (a) stage I; (b) stage II; (c) stage III; and (d) stage II', prepared from perennial *Arabis alpina* Pajares (Paj, wild type), its *perpetual flowering 1-1* (*pep1-1*) mutant derivative and annual *Arabis montbretiana* (*A. mont.*) in the perennial zone (PZ) and the annual zone (AZ). Anatomy investigated following FCA staining: in blue, staining of non-lignified cell walls (parenchyma, phloem and meristematic cells); in red, staining of lignified cell walls; and in greenish color, staining of suberized cell walls (xylem, sclerenchyma and cork). Starch, visualized following Lugol's iodine staining, is indicated in dark violet-black. Lipids, detected by Sudan IV staining, give an orange pinkish color to lipid bodies and a yellowish color to suberized and lignified cell wall structures. Black triangles: starch and lipid bodies. Abbreviations used in microscopic images: c, cork; ca, cambium; co, cortex; e, epidermis; pd, phelloderm; pe, periderm; ph, phloem, including primary phloem, secondary phloem and phloem parenchyma; pi, pith; pp, secondary phloem parenchyma; s, sclerenchyma; x, xylem, including primary xylem, secondary xylem and xylem parenchyma. Arrows point to respective tissues. Scale bars: 50 μm.

PZ. Cortical and epidermal cells were compressed and showed lignification (appearing reddish with FCA staining, Figure 3b). At stage III, lateral branches of Paj flowered and formed green siliques, and those of *pep1-1* were in a more advanced reproductive state and already senescent (Figure 2b). Secondary growth was further progressed in the PZ (PZ in Figure 3c). The lower lateral stem internodes of Paj and *pep1-1* had hardly any outer cortex left and, if present, the cortex cells were compressed. Frequently, the sclerenchyma, outer cortex and epidermis peeled off as fibers during preparation. The cambium had formed a large ring of secondary phloem and secondary xylem with parenchyma. The upper lateral stem internodes of the AZ showed the annual growth pattern (AZ in Figure 3c). Interestingly, in the AZ, interfascicular cambium and a ring of phloem parenchyma adjacent to the fascicular phloem were found in both Paj and *pep1-1* (visible for Paj in stage III, Figure 3c, but only visible between stages II and III for *pep1-1*, Figure S3a). This interfascicular cambium and phloem parenchyma were no longer visible at later stages of AZ development, but instead sclerenchyma tissue had formed, suggesting that cambium and phloem parenchyma had transformed into sclerenchyma in AZ (visible at stage III for *pep1-1*, Figure 3c, but only visible later than stage III for Paj, Figure S3b). The pith regions became hollow in the two lines, and upper stem regions began to senesce. The border of the PZ and the AZ coincided with a transition region with short internodes. Phloem parenchyma and cork gradually became narrower, until they were no longer apparent (Figure S3c,d). At stage II', lateral branches of Paj retained their vegetative character and consisted only of PZ internodes (Figure 2b). Contrary to that, lateral branches of *pep1-1* formed the AZ and flowered. Secondary growth was advanced in the PZ, comparable with stage III (PZ, Figure 3d). The upper AZ (present only in *pep1-1* and not in Paj) again showed primary growth (AZ, Figure 3d). *Arabis montbretiana* plants formed lateral branches and were marked by green siliques (Figure 2b). Lateral stems of *A. montbretiana*, only available at stage II', showed primary growth (AZ in Figure 3d). Only in a very thin zone close to the main stem was secondary growth apparent in the lateral stems of *A. montbretiana*, presumably needed for stability (Figure S3e).

Taken together, the characteristic zonation into an upper reproductive and senescent annual growth zone, the AZ, and a lower vegetative perennial growth zone, the PZ, with secondary growth is a property of perennial *A. alpina* Paj and *pep1-1*, not affected by perpetual flowering and vernalization. This zonation was absent in the annual *A. montbretiana*.

Starch and lipids are stored in secondary growth tissues of the PZ

Secondary growth in the PZ of lateral stems might be linked to nutrient storage. We investigated the deposition

of C-storage biopolymers starch and lipids, in the form of TAGs, by staining tissue sections and biochemical quantification (Figures 3 and 4). To deduce the importance of the PZ for nutrient storage during secondary growth, we investigated whether there was an increase of C-storage products from stage I (prior to visible secondary growth) to stages II or II' (evident secondary growth) during the development of the PZ. We also investigated the difference between the PZ and the AZ, which was possible at stage II' for *pep1-1* and at stage III for Paj and *pep1-1*. To support the relevance of the PZ for long-term storage, we compared the starch contents of the PZ and the AZ with starch quantified in the leaves (Figures 4a and S4).

Starch was hardly detectable at stage I in the PZ in Paj and *pep1-1* (Figure 3a), whereas it was present in the ring of secondary phloem parenchyma at stages II and II' (Figure 3b). Starch contents increased between stages I and II, by fivefold in Paj and by fourfold in *pep1-1*, as well as between stages I and II', by 10-fold in Paj and fivefold in *pep1-1* (Figure 4a). The accumulation of starch during PZ development from stages I to II indicates storage related to secondary growth. At stage III, starch was also present in secondary phloem parenchyma of the PZ in Paj and *pep1-1* (Figures 3c and 4a). In the AZ, starch was detected in the outer cortex of Paj but was hardly detected in *pep1-1* (Figure 3c). At this stage, starch contents were higher in AZ than in PZ in Paj but were lower in *pep1-1* (Figure 4a). As AZ development was advanced in *pep1-1* compared with Paj, we concluded that starch was consumed and degraded as senescence progressed in the AZ. At stage II', starch was confined to the outer cortex of the AZ in *pep1-1* and *A. montbretiana* (Figure 3d), and the content was higher than in the PZ of *pep1-1* at this stage (Figure 4a). In comparison, photosynthetically active green leaves, harvested at the same stage as lateral stem samples, had higher starch contents than corresponding PZs (compare Figure 4a with Figure S4). Green leaf starch content corresponded to transitory starch, as harvested senescent leaves had starch contents that were equal or lower than those of the PZs of Paj and *pep1-1* (compare Figure 4a with Figure S4). The localization of starch together with other molecules support the idea of the storage properties of the PZ.

The lipid staining patterns were similar but not identical to the starch staining patterns. The main difference was that in the PZ, lipid bodies were found in all stages in the secondary phloem parenchyma and, in addition, also in the secondary phloem, secondary xylem and the cambium (Figure 3a–d). In the AZ, lipid bodies were present in the outer cortex and, in addition, were found in the phloem and cambium of vascular bundles in Paj, *pep1-1* and *A. montbretiana* (Figure 3c,d). TAG contents increased in Paj from stage I to stages II and II', whereas in *pep1-1*, the

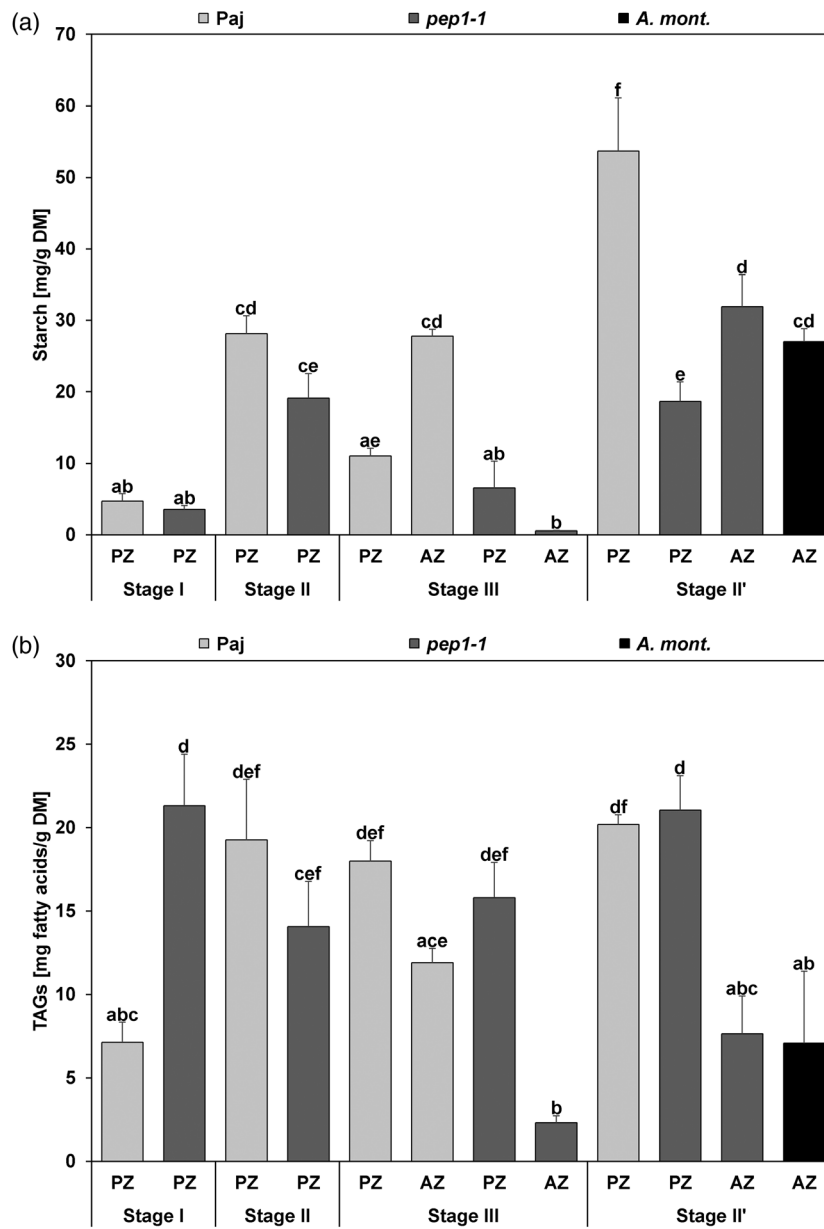


Figure 4. Contents of carbon-containing storage compounds in lateral stem internodes. Stem diagrams represent contents per dry matter (DM) of: (a) starch; and (b) triacylglycerols (TAGs). Lateral stem internodes were harvested at stages I, II, III and II', corresponding to the perennial zone (PZ) and the annual zone (AZ) of *Arabis alpina* Pajares (Paj, wild type), its *perpetual flowering 1-1* (*pep1-1*) mutant derivative and annual *Arabis montbretiana* (*A. mont.*). Data are represented as means \pm SDs ($n = 3-7$). Different letters indicate statistically significant differences, determined by one-way ANOVA and Tukey's HSD test ($P < 0.05$).

TAG contents were high at stage I and then decreased at stage II or remained constant at stage II' (Figure 4b). In all AZ samples, TAG contents were lower than in the corresponding PZ samples, in agreement with anatomical observations (Figure 4b), showing that the PZ is a TAG storage location.

In summary, tissues derived from secondary growth play a predominant role in C storage in the form of starch and TAGs in PZ. As this was also the case in *pep1-1*, nutrient storage occurs irrespective of flowering and vernalization.

Carbon storage is reflected by carbon/nitrogen (C/N) ratio

An elevated C level and C/N ratio is an indicator for carbon storage. Total C contents may also reflect storage properties. They rose in Paj and *pep1-1* from stages I to II and then II' (Figure 5a). Total C contents were lower in the AZ compared with the PZ at stage III in *pep1-1*. The decrease was not significant in the case of Paj at stage III and in the case of *pep1-1* at stage II', however (Figure 5a). Total N contents changed in an opposite pattern to C contents and

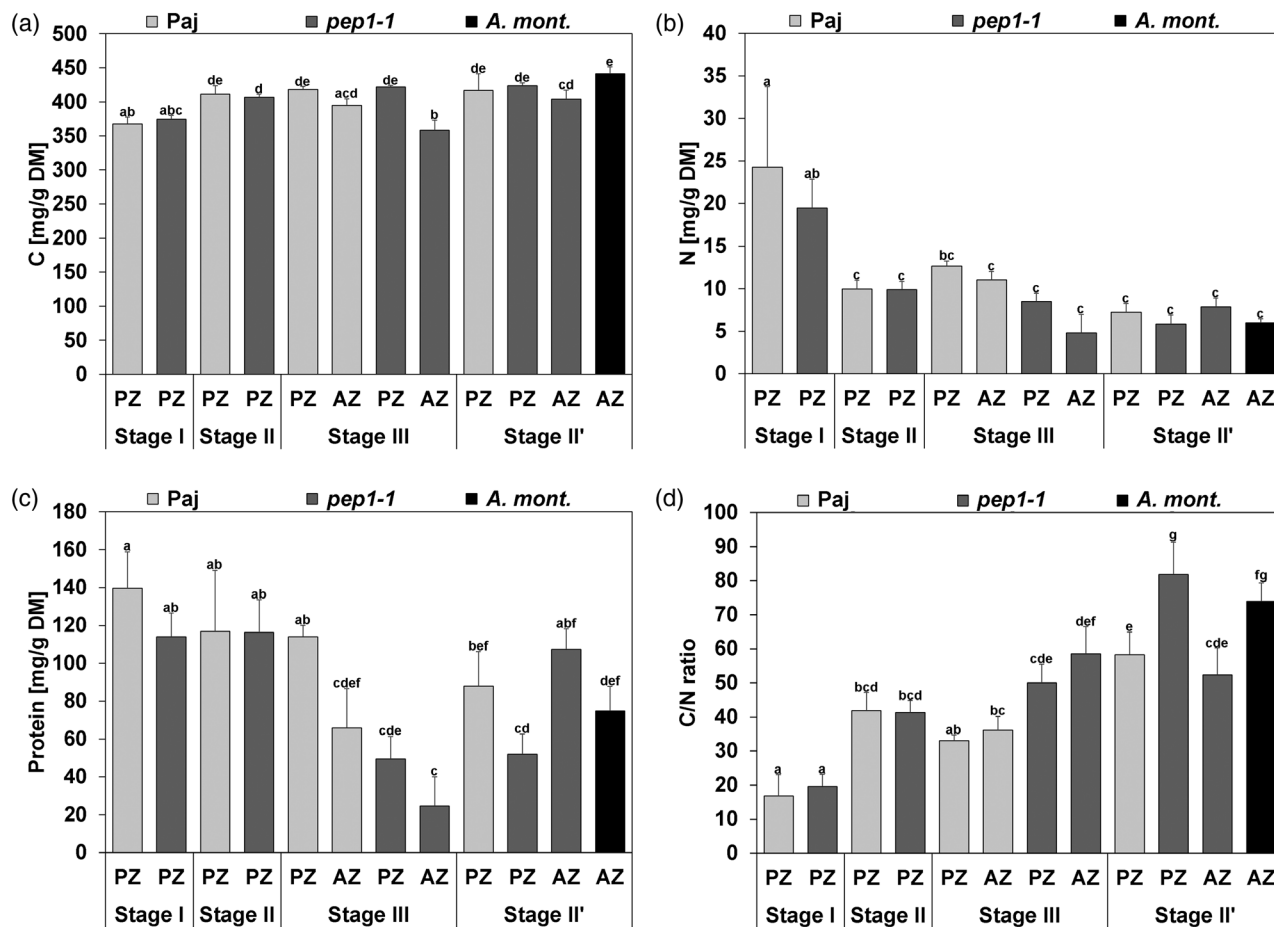


Figure 5. Carbon, nitrogen and protein contents in lateral stem internodes. Stem diagrams represent contents per dry matter (DM) of (a), carbon (C), (b), nitrogen (N), (c), protein, (d), C/N ratios. Lateral stem internodes were harvested at stages I, II, III and II', corresponding to perennial zone (PZ) and annual zone (AZ) of *Arabis alpina* Pajares (*Paj*, wild type), its *perpetual flowering 1-1* (*pep1-1*) mutant derivative and annual *Arabis montbretiana* (*A. mont.*). Data are represented as mean \pm SD ($n = 3-7$). Different letters indicate statistically significant differences, determined by one-way ANOVA-Tukey's HSD test ($P < 0.05$).

decreased significantly from 20–25 mg g⁻¹ dry mass at stage I to 5–10 mg g⁻¹ dry mass at stages II and II', and then remained at a constant low level in stage III (Figure 5b). This finding discounts the action of N-storage compounds. Total protein contents were highest, with 110–140 mg g⁻¹ dry mass in stages I and II, in the PZ of *Paj* at stage III, whereas they were lower and varied between the AZ and the PZ and between lines without any apparent pattern at stages III and II' (Figure 5c). Perhaps the lower N contents indicate a lower metabolic activity of the fully developed PZ. The C/N ratios were lowest at stage I and were increased at stages II, III and II'; however, no distinction could be made between the PZ and the AZ, and no noticeable differences between the lines were observed (Figure 5d). The C-storage capacity of the PZ and possible turnover of C-storage compounds during flowering is reflected by the C/N ratio of the PZs of *Paj* at stages III and II'. The C/N ratio of the PZ retaining vegetative character at stage II' was significantly higher than that of the PZ corresponding to flowering at stage III. Compared with stems,

roots may also serve as a C-storage reservoir; however, in this case TAGs would be the primary C-storage products and not starch (Figure S5).

Taken together, the total C content increased slightly as the development of the PZ progressed. This slight increase reflects the storage of starch and TAGs but may also include increases in cell walls.

Hormones affect secondary growth in lateral stems

We tested the effects of hormone application to internodes in a juvenile PZ stage prior to visible secondary growth. First, we applied synthetic 6-benzylaminopurine (BAP) for 8 or 46 days to PZ and AZ internodes, respectively. In the PZ, cambium and phloem parenchyma regions were increased in width (Figure 6a,b, 'Anatomy'). The increase in width corresponded to a doubling of cambium cells from two to about four cells and an additional one or two cells of phloem parenchyma in the fascicular and interfascicular regions (Figure 6a–d). Interestingly, the increase in width was also found in the newly developed second

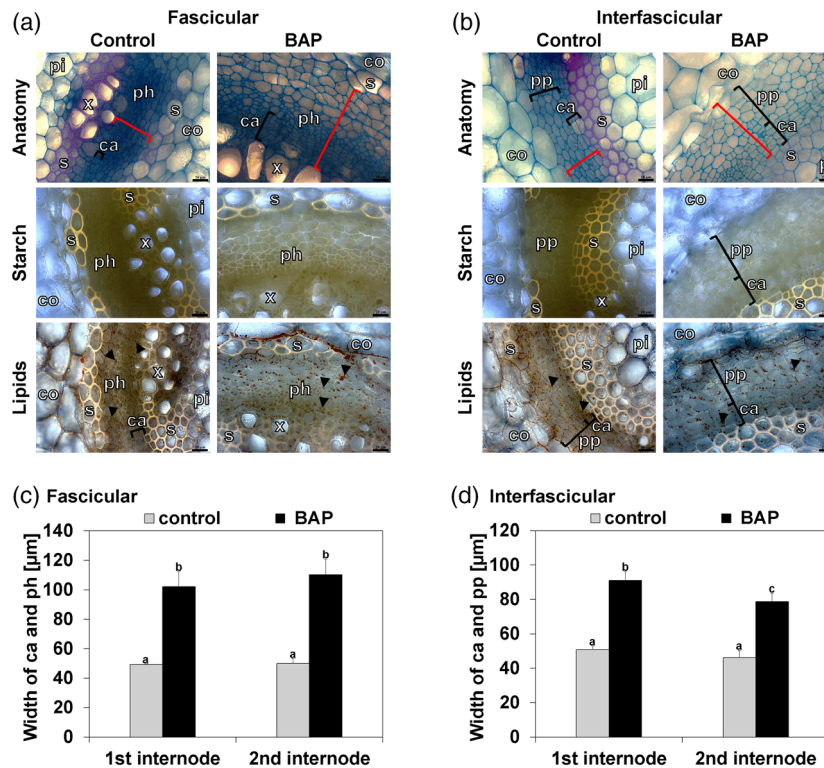


Figure 6. Effect of cytokinin treatment on cambium activity in the perennial zone (PZ). (a, b) Lateral stem first internode cross sections of: (a) the fascicular region; and (b) the interfascicular region of *Arabis alpina* *perpetual flowering 1-1* (*pep1-1*) mutant, following treatment with cytokinin (2 mM 6-benzylaminopurine, BAP) or mock control for eight days to the first internode. Representative images are shown. Anatomy investigated following FCA staining: in blue, staining of non-lignified cell walls (parenchyma, phloem and meristematic cells); in red, staining of lignified cell walls; and in greenish color, staining of suberized cell walls (xylem, sclerenchyma and cork). Starch, visualized following Lugol's iodine staining, is indicated in dark violet–black. Lipids, detected by Sudan IV staining, give an orange pinkish color to lipid bodies and a yellowish color to suberized and lignified cell wall structures. Black triangles, lipid bodies; black brackets, responsive cambium and phloem/secondary phloem parenchyma; red brackets, quantified tissue width in (c) and (d). Abbreviations used in microscopic images: c, cork; ca, cambium; co, cortex; e, epidermis; pd, phelloderm; pe, periderm; ph, phloem including primary phloem, secondary phloem and phloem parenchyma; pi, pith; pp, secondary phloem parenchyma; s, sclerenchyma; x, xylem, including primary xylem, secondary xylem and xylem parenchyma. Scale bars: 20 µm. (c, d) Quantified cambium and phloem/secondary phloem widths in (c) fascicular and (d) interfascicular internode regions for first and second internodes. Data are represented as means \pm SDs ($n = 3$). Different letters indicate statistically significant differences, determined by one-way ANOVA and Tukey's HSD test ($P < 0.05$).

internodes that had not been treated with BAP directly, showing that a cytokinin-induced signal acted in the adjacent internode (Figure 6c, d). Similar to the control plants, starch did not accumulate in the secondary phloem parenchyma of the treated plants. Patterns of lipid bodies were similar in treated and control stems (Figure 6a,b, 'Starch' and 'Lipids'). After 46 days of BAP treatment, the AZ internodes also increased in width (Figure S6b). Additionally, flowering was delayed and a second zone with short internodes, as found in the PZ–AZ transition zone, was formed two to three internodes above the first (Figure S6b). Cambium and phloem parenchyma regions were considerably increased in width in the AZ (Figure 7a–d, 'Anatomy'). Secondary phloem parenchyma was formed in the interfascicular regions of 'Top' and 'Middle' areas of the AZ. In the control, the corresponding areas would differentiate into sclerenchyma (Figure 7b,d, 'Anatomy', 'Top' and 'Middle'). Furthermore, cork cambium and cork were formed in the 'Middle' area in the fascicular and

interfascicular regions of the treated stems (Figure 7a,b). A difference with regards to starch accumulation was observed only for the 'Bottom' area (Figure 7a,b, 'Starch', 'Bottom'). Starch accumulated in secondary phloem parenchyma in the treated AZ stems, whereas starch was not observed in the corresponding tissue of the control. The observed starch accumulation in the AZ supports the strong involvement of cytokinins in the development of the perennial stem with a storage function. Patterns of lipid bodies were similar between treated and untreated stems in cambium and phloem parenchyma (Figure 7a,b, 'Lipids').

Upon application for 8 days, auxin (1-naphthaleneacetic acid, NAA), gibberellic acid (GA_3) and ethylene precursor (1-aminocyclopropane-1-carboxylic acid, ACC) also influenced cambial activity in the first internode of the PZ. Cambium and phloem parenchyma regions were increased in width but, in contrast to BAP, to a maximum of 30%, and only in the treated first internode but not in the second

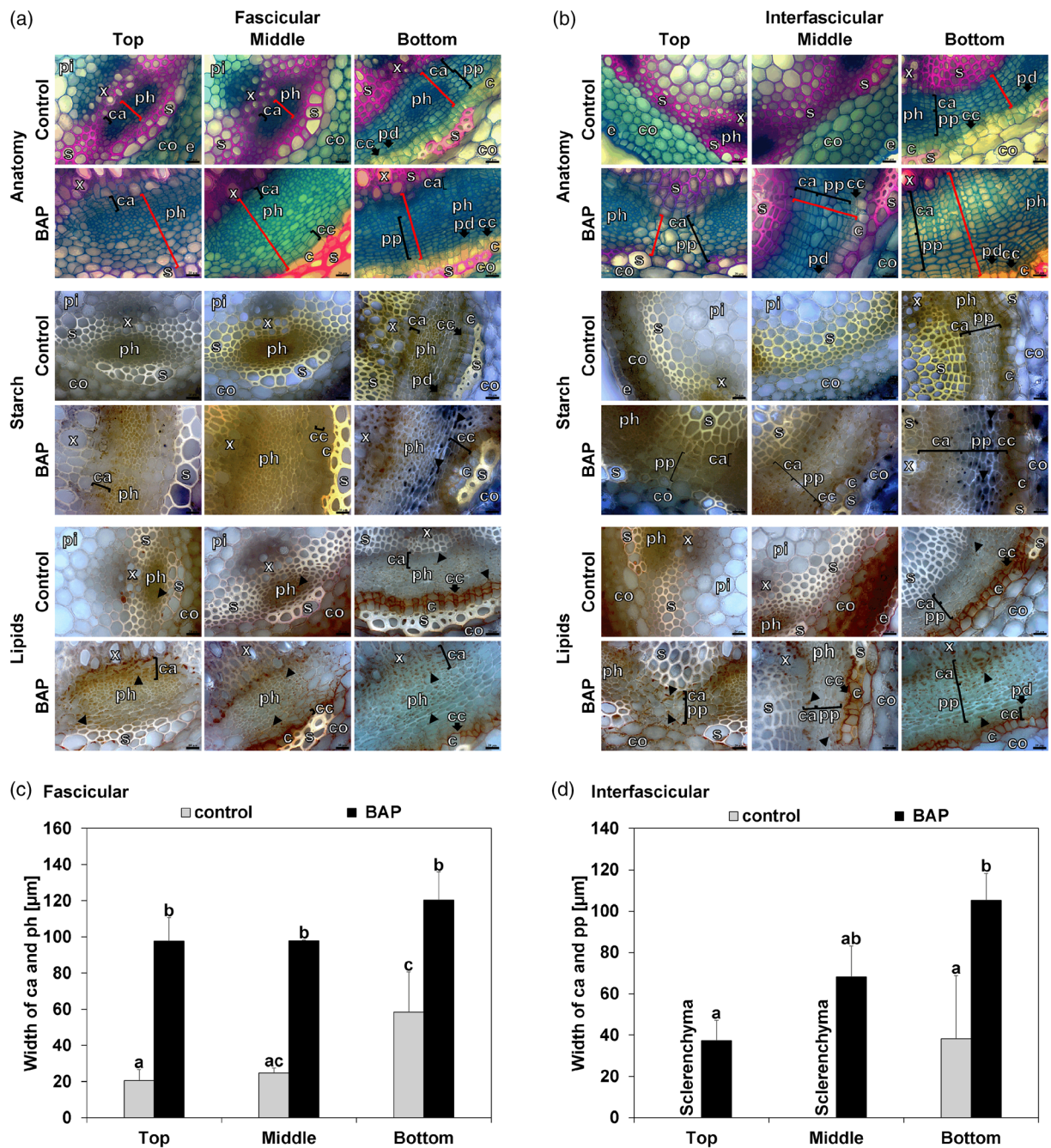


Figure 7. Effect of cytokinin treatment on cambium activity in the annual zone (AZ). (a, b) Lateral stem internode cross sections of top, middle and bottom parts of the AZ (see also Figure S6) in: (a) the fascicular region; and (b) the interfascicular region of *Arabidopsis thaliana* *perpetual flowering 1-1* (*pep1-1*) mutant, following the treatment of all developing internodes of the AZ with cytokinin (2 mM 6-benzylaminopurine, BAP) or mock control for 46 days. Representative images are shown. Anatomy investigated following FCA staining: in blue, staining of non-lignified cell walls (parenchyma, phloem and meristematic cells); in red, staining of lignified cell walls; and in greenish color, staining of suberized cell walls (xylem, sclerenchyma and cork). Starch, visualized following Lugol's iodine staining, is indicated in dark violet-black. Lipids, detected by Sudan IV staining, give an orange pinkish color to lipid bodies and a yellowish color to suberized and lignified cell wall structures. Black triangles, starch and lipid bodies; black brackets, responsive cambium and phloem/secondary phloem parenchyma; red brackets, quantified tissue widths in (c) and (d). Abbreviations used in microscopic images: c, cork; ca, cambium; co, cortex; e, epidermis; pd, phelloderm; pe, periderm; ph, phloem, including primary phloem, secondary phloem and phloem parenchyma; pi, pith; pp, secondary phloem parenchyma; s, sclerenchyma; x, xylem, including primary xylem, secondary xylem and xylem parenchyma. Scale bars: 20 µm. (c, d) Quantified cambium and phloem/secondary phloem widths in (c) fascicular and (d) interfascicular internode regions in top, middle and bottom parts of the AZ. Data are represented as means ± SDs (n = 3). Different letters indicate statistically significant differences, determined by one-way ANOVA and Tukey's HSD test (P < 0.05).

(Figures S7–S9). No changes with regard to starch and lipid body accumulation patterns were observed in the first and second internodes of the PZ following the hormone treatments, indicating again that starch and lipid body accumulation in the PZ is not an immediate effect of hormone supply (Figures S7–S9).

Taken together, among the hormones tested cytokinin had the highest effect on secondary growth in the PZ. The application of cytokinin to the AZ caused a shift in the zonation pattern and promoted secondary growth in the AZ, indicating that cytokinins act as signals to induce secondary growth. At the early growth stage starch accumulation was not stimulated by cytokinins, whereas starch accumulation was stimulated after prolonged treatment.

Transcriptome analysis reflects cytokinin effects in the PZ

To provide support for PZ and AZ activities and obtain hints about signaling, we conducted a gene expression profiling experiment with *pep1-1* lateral stem internodes using RNA-seq at 4- and 5-week-old juvenile developmental PZ stages (stage I_PZ and stage II_PZ), a 7-week-old PZ stage with secondary growth and lipid bodies (stage III_PZ), and a 30-week-old mature PZ stage (stage IV_PZ) with advanced secondary growth and accumulated starch and lipid bodies and AZ internodes, either in close proximity to the formed inflorescence (stage IV_AZ_if) or in the region with short internodes of the AZ (stage IV_AZ_si) (Figure 8a; Table S2). Hierarchical clustering (HC) and principal component analysis (PCA) confirmed the close relationships of three biological replicates of each sample and the quality of the RNA-seq data (Figure S10). In HC, four distinct clusters were apparent, one cluster with stages IV_AZ_si and IV_AZ_if, a second cluster with stages I_PZ and II_PZ, grouping closely with AZ samples. The third and fourth cluster were stages III_PZ and IV_PZ, whereby the fourth cluster was most distant from all other groups (Figure S10a). PCA analysis confirmed the expected variation between the samples. PC1 separated between the age of the internodes, similar to the first clusters in HC, whereas PC2 grouped according to PZ and AZ (Figure S10b).

As we were seeking gene expression differences between the PZ and the AZ, we conducted meaningful crosswise enrichment analysis of gene ontology (GO) terms (Tables S3–S17). Cytokinin terms were enriched in comparisons of stages II_PZ and IV_AZ_if, III_PZ and IV_AZ_si or IV_AZ_if (Tables S11, S13 and S14). By grouping the data and comparing all PZ with all AZ stages, enrichment analysis resulted in a total of 48 PZ- and 89 AZ-enriched GO terms, with cytokinin-related terms among them (Figure 8b; confirmed by gene expression validation in Figure 9; Tables S18 and S19;). Other PZ-enriched GO terms were related to organ and shoot development, nutrient response and starvation genes, and other hormone

responses (Figure 8b; Table S18). AZ-enriched terms were cell wall, carbohydrate metabolism and photosynthesis categories (Figure 8b; Table S18). GA biosynthesis and response terms were enriched in AZ (Figure 8b; Table S18).

In summary, the PZ shows high responsiveness to cytokinins as compared with the AZ, confirming that cytokinins play an important role in the differentiation of the PZ.

DISCUSSION

The complex perennial lifestyle of *A. alpina* comprises an allocation of nutrients and the storage of high-energy C compounds in the proximal vegetative perennial zone (PZ), characterized by secondary growth. The distal inflorescence annual zone (AZ) remains in a primary growth stage.

***Arabis alpina* stems have proximal perennial and distal annual zones, with C sequestration in the cambium and derivatives in the perennial zone**

The vegetative growth zone (V) coincided with the PZ characterized by secondary growth, whereas the distal inflorescence zone (I) represented the AZ with primary growth. In the PZ–AZ transition zone, secondary growth gradually shifted to primary growth. At the beginning of stem development, the anatomy of stem cross sections was similar in the PZ in *A. alpina* and the AZ of *A. alpina* and *A. montbretiana*. As development continued, secondary growth was initiated by the activities of cambium and then cork cambium. At the bottom of annual stems in *A. montbretiana* secondary growth was also found, where it may serve to provide general stability of upright stems, as described in *Arabidopsis thaliana* (Agusti *et al.*, 2011). Moreover, the perennial life strategy is regarded to be ancestral (Hu *et al.*, 2003; Grillo *et al.*, 2009). Secondary growth at the bottom of *A. montbretiana* stems may still occur to some extent through the evolutionary history of the annual derived from a perennial ancestor. In the AZ, the interfascicular cambium and inner layer of the cortex differentiate into sclerenchyma as development progresses, perhaps for stabilization during flowering and silique production. The occurrence of PZ and AZ regions in all stems in the *A. alpina* wild type Paj and *pep1-1* suggests that the genetically encoded signals for the PZ–AZ transition do not require vernalization treatment. Instead, we propose that heterochronic regulation might control it, as discussed later.

Perennials must use a perennating storage place to remobilize nutrients in a new growth season. Several criteria designate the secondary growth zone as a storage organ in *A. alpina*. First, the PZ accumulates high C-storage compounds during its development between stages I and II (and II'). Second, this occurs in cambium and/or cambium-derived tissues known to be coupled to the storage of nutrients in trees. Third, the PZ is perennial, which is a

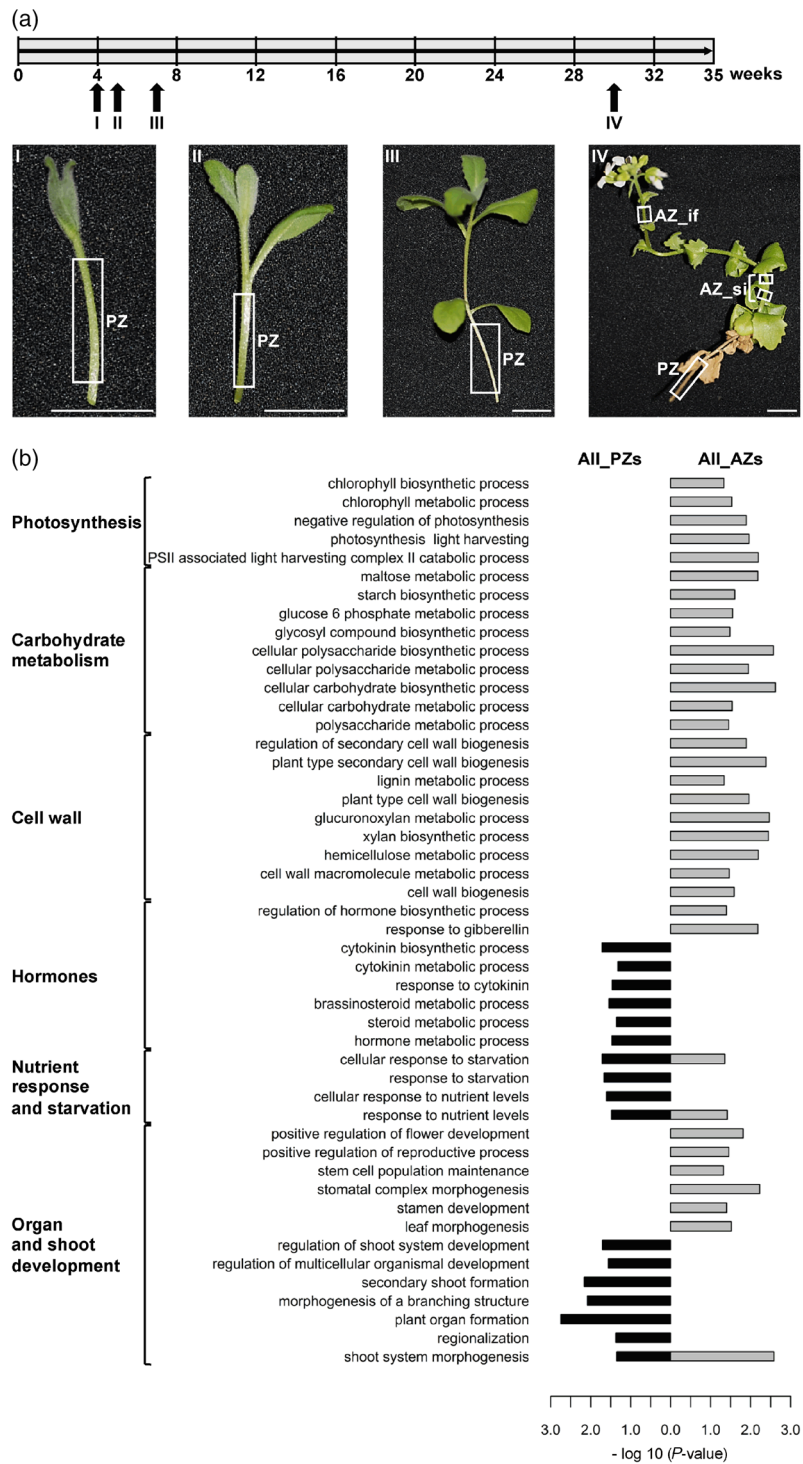


Figure 8. Transcriptome analysis of perennial (PZ) and annual (AZ) lateral stem zones. (a) Plant growth and morphology. Upper part, plant growth scheme and harvesting stages I–IV for RNA-sequencing (RNA-seq), grown under long-day conditions at 20°C, for the *Arabis alpina perpetual flowering 1-1* (*pep1-1*) mutant. Bottom part, lateral stem morphology at each harvesting stage. White rectangles in representative photos indicate parts harvested at: stage I_PZ and stage II_PZ, both prior to visible secondary growth in the juvenile phase; stage III_PZ and stage IV_PZ, PZ, with visible secondary growth; stage IV_AZ_si, small internode region; and stage IV_AZ_if, inflorescence region. Scale bars: 1 cm. (b) GO term enrichment analysis of the PZ versus the AZ. The PZ comprised the sum of stages I–IV_PZ, whereas AZ comprised stage IV_AZ_si and IV_AZ_if combined. GO terms were assigned to the indicated categories of photosynthesis, carbohydrate metabolism, cell wall, hormones, nutrient response and starvation, and organ and shoot development. Enrichment ($P < 0.05$) represented as $-\log_{10}$ values. Further information about the GO term enrichment analysis in Table S18.

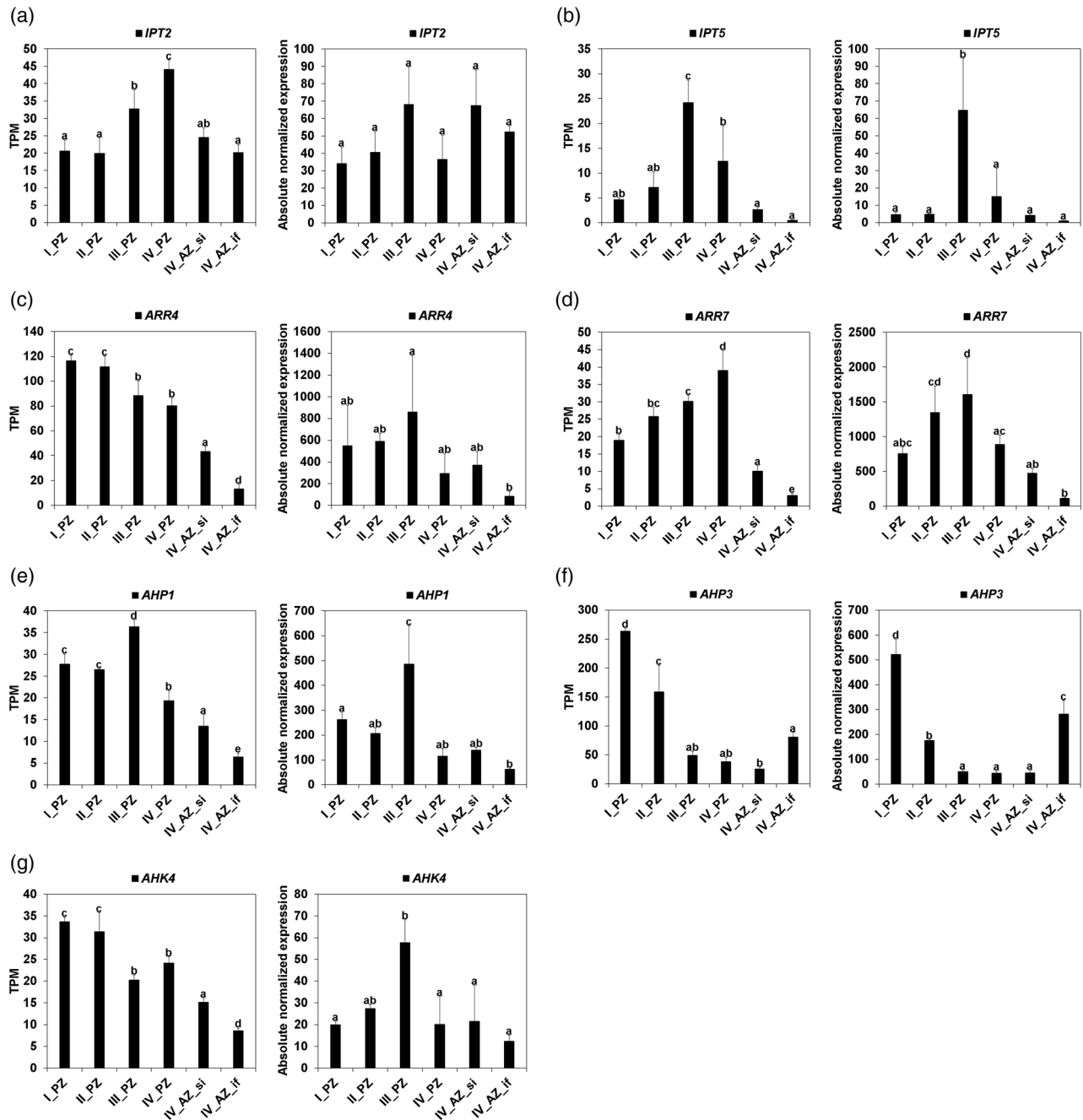


Figure 9. Gene expression of orthologs of Arabidopsis cytokinin biosynthesis and response genes in lateral stem internodes. Gene expression was tested at different stages of the development of the perennial zone (PZ) and the annual zone (AZ) in *Arabis alpina* *perpetual flowering 1-1* (*pep1-1*) mutant derivative. Represented are RNA-sequencing data (left; TPM, transcripts per million) and reverse transcription-qPCR data (right; absolute normalized expression): (a) *IPT2*, ISOPENTENYLTRANSFERASE 2; (b) *IPT5*, ISOPENTENYLTRANSFERASE 5; (c) *ARR4*, ARABIDOPSIS RESPONSE REGULATOR 4; (d) *ARR7*, ARABIDOPSIS RESPONSE REGULATOR 7; (e) *AHP1*, ARABIDOPSIS HISTIDINE-CONTAINING PHOSPHOTRANSMITTER 1; (f) *AHP3*, ARABIDOPSIS HISTIDINE-CONTAINING PHOSPHOTRANSMITTER 3; and (g) *AHK4*, ARABIDOPSIS HISTIDINE KINASE 4. Data are represented as means \pm SDs ($n = 3$). Different letters indicate statistically significant differences, determined by one-way ANOVA and Tukey's HSD test ($P < 0.05$).

prerequisite for storage rather than transitory accumulation. Fourth, there is GO term enrichment of nutrient response and starvation, indicative of a sink. All four criteria are met by the PZ, whereas only the first is met by the AZ. In two instances starch was higher in the AZ than in

the PZ (*pep1-1* at stage II'; Paj at stage III). Here, starch was present in the outer cortex. This starch is rather transitory starch from photosynthesis, and this could be the reason for the lack of starch biosynthesis term enrichment in the PZ. Starch contents in leaves are higher in green leaves,

compared with the PZ, whereas they are as low or lower in senescent leaves. This indicates that starch is formed as transitory starch in green leaves in *A. alpina* and presumably also in the AZ. In contrast, the TAG content in these two situations was lower in the AZ than in the PZ in Paj at stage III and in *pep1-1* at stage II', again supporting the storage function.

The N pool in *A. alpina* stems coincided with the protein pool, noteworthy in the early PZ but decreasing with development. Thus, N storage is not likely. Instead, the PZ with cambium and cambium derivatives functions as a carbon nutrient storage reservoir in *A. alpina*. Secondary stem growth is also associated with nutrient storage in trees (reviewed by Furze *et al.*, 2018), where it occurs in pith cells, wood ray and bark parenchyma (Netzer *et al.*, 2018). Other perennating storage organs are not formed. Roots do not match the criteria of nutrient storage. Neither do leaves that have transitory starch and senesce.

Cytokinins are signals for the demarcation of annual and perennial growth zones

The open question is which events are responsible for demarcating the sharp PZ–AZ transition. Besides secondary and primary growth and C storage, the PZ–AZ boundary also separates organ differentiation at the nodes and in axils, such as bud outgrowth into fully developed lateral stems, bud dormancy, bud differentiation into a singular flower or bud outgrowth into flowering secondary and tertiary branches. The small PZ–AZ transition zone has short internodes and is marked by a gradual shift from secondary to primary growth. Multiple signals could act in these differentiation processes in the PZ and AZ.

One possible explanation is that the PZ state is an initial ground state. In this scenario, the progression to the PZ becomes halted later in developmental time in the AZ. In this model, the PZ–AZ transition is a heterochrony or developmental phase transition. As the regulation of bud fate is under the control of meristem identity genes, mutants in the genes affect developmental phase transitions. In annuals, some progression to the PZ may take place in a rudimentary manner at the bottom of stems or during the onset of senescence for stabilization reasons. A full progression to the PZ is prevented, however. We exclude that flowering or vernalization emit signals for the PZ–AZ transition in Paj and *pep1-1*. The *pep1-1* mutant also has the PZ–AZ transition. Even though the presence of flowers was not a requirement for the PZ–AZ transition, upstream regulators of flowering and developmental phase transition, namely the regulatory network of microRNA miR156, SPL proteins and Mediator complex subunits, may well control aspects of stem differentiation (Park *et al.*, 2017; Bergonzi *et al.*, 2013; Guo *et al.*, 2017; Hyun *et al.*, 2019; Zhang and Guo, 2020).

Developmental decisions are often taken under the influence of plant hormones and they affect stem differentiation, flowering and developmental phase transition. The application of cytokinin shifted the PZ–AZ transition and might be coupled to a heterochronic signal. A cytokinin effect was further confirmed by the enrichment of cytokinin biosynthesis and response gene expression in the developing PZ. Even direct application to the AZ caused an extension of the PZ into the AZ. Thus, cytokinins might be signals that promote progression during developmental phase transitions, and cytokinin depletion rather than decreased sensitivity might trigger the precocious halting in AZ. Cytokinins also play a crucial role in the regulation of source and sink relationships, including starch deposition, although to our knowledge this was not reported in the perennial *Populus* model species (Thomas, 2013). Cytokinins are signals likely to promote secondary growth in the PZ and later, in combination with flowering and senescence, also promote sink activity and starch formation. That cytokinin-promoted nutrient deposition might be coupled to secondary growth is supported by our observation of starch accumulation in the proximal AZ region with increased secondary phloem parenchyma formation affected by the application of cytokinin. Cytokinins also retard senescence, which is partly explained by cytokinin-modified source–sink relationships (Thomas, 2013). Together, this suggests that cytokinins are less likely to act in the AZ but instead contribute to the maintenance of the adult vegetative state in the PZ.

Gibberellin (GA), auxin and ethylene also promote secondary growth in the PZ, yet these hormones acted only locally on the same internode and not to the same extent as cytokinin. Auxin produced in V3 lateral branches may cause bud dormancy in V2, according to an auxin canalization model. This growth inhibition effect is also under the control of vernalization and is further promoted by enhanced sinks for nutrients in the AZ and V3 lateral branches (Vayssières *et al.*, 2020). In our experiments, auxin did not stimulate secondary growth in the neighboring internodes that had not been treated in the way that cytokinin did. Auxin signaling may give rise to distinctive V subzones in the PZ but not in the PZ–AZ transition. GAs are influential in the xylem region, promoting xylem cell differentiation and lignification (Denis *et al.*, 2017). Interestingly, this stronger lignification of vascular cells resembles anatomy that has been detected in our study in the AZ of Paj and *pep1-1*, as well as in *A. montbretiana* at later developmental stages. Perhaps GA signals explain the tendency of the cambium in the AZ to develop lignified cell walls and differentiate into sclerenchyma. Indeed, GA-related GO terms were enriched in AZ versus PZ, supporting this idea.

To test whether hormone gradients and developmental phase transition regulation are responsible for the

transition from secondary to primary growth, transgenic approaches will be helpful in the future to manipulate these responses in the different growth zones.

CONCLUSIONS

The functional complexity of stem differentiation in *Arabis* offers the possibility to study the regulation of perennial (advanced secondary growth and storage) and annual (primary growth and senescence) traits using the same model species. The close relationship among Brassicaceae and the similarities of secondary growth processes in trees and *Arabidopsis* can be exploited to unveil signaling pathways and regulators for stem differentiation in *A. alpina* in future projects. Further studies need to show whether heterochronic PZ–AZ transition genes and plant hormones determine the transport of effectors, the sensitivity to respond to effectors or alter specific long-distance signaling processes, and how these processes link flowering control and secondary growth.

EXPERIMENTAL PROCEDURES

Plant material, growth conditions and plant harvesting

Perennial *A. alpina* wild type Pajares accession (Paj), perpetual flowering mutant *pep1-1* (Wang *et al.*, 2009) and annual *A. montbretiana* (Kiefer *et al.*, 2017) plants were grown on potting soil (Vermehrungssubstrat; Stender GmbH, <https://www.stender.de/de-de>) with a humidity of 70% in a plant growth chamber (Percival Scientific; CLF Plant Climatics, <https://www.plantclimatics.de>) under controlled long-day (16 h of light and 8 h of dark, at 20°C) or short-day (8 h of light and 16 h of dark, at 4°C for vernalization) conditions and harvested at stages I, II, III and IV, as described in the Results section and corresponding figures. Plants were fertilized every second week using universal Wuxal (Aglukon, <https://www.aglukon.com>). All experiments were performed with between three and seven biological replicate plants, as indicated in the text. For anatomical analysis, between four and 11 internode cross sections were prepared per lateral stem sample and stored in 70% ethanol (Figure S1).

Biochemical analysis was conducted with lateral stems from nodes 1–5 of the main axis in the case of Paj and *pep1-1*, or from all lateral stems of *A. montbretiana*. Internodes of one plant were dissected and pooled as one biological replicate, deep frozen in liquid nitrogen and stored at –80°C. Entire root systems of single plants were harvested as one root sample and residual soil was removed. Green and senescent leaves from lateral stems were pooled separately per plant as one biological replicate each. All plant samples were harvested in the middle of the day for comparison between each other, freeze-dried, lyophilized and ground to fine powder in a mixer mill (Mixer Mill MM 200; Retsch, <https://www.retsch.com>). All biochemical measurements were conducted with the same plant samples (Figure S1).

For hormone treatments, *pep1-1* plants were grown as above under long-day conditions for between 4 and 5 weeks. The two lateral branches with one elongated internode in a juvenile PZ stage were treated with 300 µl of either 2 mM BAP, 0.5 mM NAA, 4 mM GA or 2 mM ACC solution (or mock treated in 50% ethanol mixed with 10 mg of lanolin and pasted with a brush along the first internode). The treatment was repeated after 4 days, and internodes were harvested after 8 days. AZ treatment was initiated

when the plants were 18 weeks old and two elongated internodes of the AZ were formed. Both internodes of five replicate plants were treated with 2 mM BAP solution, as described above. The treatment was performed for 46 days until the siliques and uppermost part of the AZ of the control plants started to senesce. Newly formed and already present internodes were treated every fourth day. Harvested AZs were divided into three regions (top, middle and bottom), comprising two or three internodes.

For RNA-sequencing (RNA-seq), 12 *pep1-1* plants were grown per biological replicate. Three biological replicates were used for each sampling stage examined, as described in the text and corresponding figures. Plant samples were immediately deep frozen in liquid nitrogen, stored at –80°C and ground to fine powder before use.

Microscopic analysis

Hand-made internode cross sections (50–100 µm) were incubated for 5–8 min in 1 mg ml^{–1} fuchsin, 1 mg ml^{–1} chrysoidine, 1 mg ml^{–1} astra blue, 0.025 ml ml^{–1} acetic acid staining (FCA staining) solution, washed in water and alcohol solutions and mounted. For starch staining, sections were incubated for 5 min in 50% Lugol solution (Sigma-Aldrich, <https://www.sigmaaldrich.com>), rinsed in water and mounted. For lipid staining, sections were incubated for 30 min in a filtered solution of 0.5% Sudan IV in 50% isopropanol, rinsed in water and mounted. Pictures were taken with an Axio Imager 2 microscope (Carl Zeiss Microscopy, <https://www.zeiss.com>), equipped with an Axiocam 105 color camera (Carl Zeiss Microscopy) using bright-field illumination. Images were processed and tissue width quantified with ZEN 2 (blue edition; Carl Zeiss Microscopy).

Starch quantification

Starch was quantified enzymatically according to Smith and Zeeman (2006). Briefly, starch was extracted by boiling 10 mg lyophilized plant material in 80% ethanol. Extracted starch granules were gelatinized at 100°C. After incubation with α-amylglucosidase and α-amylase the samples were assayed for glucose in a microplate reader (Tecan, <https://www.tecan.com>) using hexokinase and glucose 6-phosphate dehydrogenase to monitor the reduction of NAD⁺ at 340 nm (extinction coefficient 6220 l mol^{–1} cm^{–1}).

Triacylglycerol quantification

Triacylglycerols (TAGs) were obtained by the fractionation of glycerolipids and quantified based on their fatty-acid contents, normalized to plant sample dry weight (Sergeeva *et al.*, 2021). Briefly, lipids were isolated from dried plant samples according to a modified acidic chloroform/methanol extraction method for glycerolipids (Hajra *et al.*, 1974; Wewer *et al.*, 2011). TAGs were separated from glycolipid and phospholipid fractions by successive elution with chloroform, acetone/isopropanol and methanol. Fatty-acid methylesters (FAMES) of the TAG fatty acids or of the total fatty acids from plant samples were analyzed by gas chromatography mass spectrometry (GC-MS) and the resulting peaks were integrated for quantification (Sergeeva *et al.*, 2021).

Protein content determination

Lyophilized plant material (10 mg) was taken up in 200 µl (for stems) or 300 µl (for roots) of Laemmli buffer (2% SDS, 10% glycerol, 60 mM Tris-HCl, pH 6.8, 0.005% bromphenol blue, 0.1 M dithiothreitol, DTT) and heated at 95°C for 10 min. Total protein contents were assayed using the 2-D Quant Kit (GE Healthcare,

<https://www.gehealthcare.com>), measuring OD₄₈₀ in a microplate reader (Tecan) using a bovine serum albumin mass standard curve.

Determination of carbon and nitrogen

For C and N quantification, 2 mg of lyophilized plant material, packed into tin containers, was applied to elemental analysis isotope ratio mass spectrometry (EA-IRMS) (Elementar Analysensysteme, <https://www.elementar.com>). C/N ratios were calculated from C and N values.

RNA isolation

Total RNA from plant samples was isolated using the RNeasy Plant Mini Kit (Qiagen, <https://www.qiagen.com>), including DNase I digestion via the RNase-Free DNase Set to remove traces of genomic DNA (Qiagen). The quality and quantity of the isolated RNA was examined with the Fragment Analyzer (Advanced Analytical Technologies GmbH, <https://www.agilent.com>). All samples had a suitable RNA quality number above 7.0 (with a mean RQN of 8.9).

RNA sequencing and analysis

RNA-seq analysis was conducted for three biological replicates per sample. For gene expression profiling, libraries were prepared using the Illumina TruSeq® Stranded mRNA Library Prep kit. Prepared libraries were sequenced on the HiSeq3000 system (Illumina, <https://www.illumina.com>) with a read set-up of 1 × 150 bp and an expected number of 28 Mio reads in the Genomics and Transcriptomics Laboratory of the Biologisch-Medizinisches Forschungszentrum (BMFZ) at HHU (<https://www.gtl.hhu.de>).

Using the latest publicly available versions of the *A. alpina* genome assembly (Arabis_alpina.MPIPZ.V5.chr.all.fasta and Arabis_alpina.MPIPZ.V5.chr.all.liftOverV4.v3.gff3, both downloaded from <http://arabis-alpina.org>), 34 220 coding sequences (CDS) were assembled. The closest *Arabidopsis thaliana* orthologs were determined by blasting *A. alpina* CDS assemblies against the most recent version of the *Arabidopsis thaliana* proteome sequences (TAIR10_pep_20101214_updated; downloaded from the Arabidopsis Information Resource, <https://www.arabidopsis.org>) using the BLASTX algorithm of the BLAST+ suite (Altschul et al., 1990) with an E-value threshold of <1E5. Among multiple resulting hits, the Arabidopsis proteins with the highest bit score followed by the lowest E value were accepted as the closest orthologs if the percentage of identity was >25% of the aligned amino acids (Doolittle, 1986) and the E value was <1E-15. Single end reads were trimmed with TRIMMOMATIC (Bolger et al., 2014) and the quality of the trimmed reads was evaluated with fastqc (Andrews, 2010). Using KALLISTO (Bray et al., 2016), the trimmed reads were mapped to the *A. alpina* CDS assemblies and quantified, which resulted in estimated counts and transcripts per million (TPM) values per gene. As a control, the trimmed reads were mapped to the genome assembly with HISAT2 (Kim et al., 2015) and transcripts were quantified with HTSEQ-COUNT (Anders et al., 2015) using a gene transfer format (*.gtf) file that was generated from the general feature format (*.gff3) file. The resulting counts were transformed to TPM and used for PCA (using PRCOMP in R) and hierarchical clustering (HC; using DIST and HCLUST in R). Estimated counts were used for statistical analysis using EDGER (Robinson et al., 2010; McCarthy et al., 2012). The resulting P values were adjusted with the Bonferroni method. Fold-change values of gene expression were calculated in pairwise comparisons between samples and pooled PZ and AZ samples. The above-described calculations were performed with the values obtained from KALLISTO and with those obtained from HISAT2 and HTSEQ-COUNT. Genes were accepted as

differentially regulated if $P < 0.01$ with both mapping and quantification methods. Graphs were produced with TPM obtained by KALLISTO. The transcriptome data set is available for download under GEO number GSE152417.

Gene ontology (GO) analysis was carried out using TOPGO (Alexa and Rahnenfuhrer, 2010) with the closest *Arabidopsis thaliana* ortholog locus IDs (AGI code) using the latest publicly available *Arabidopsis thaliana* GO annotations (go_ensembl_arabidopsis_thaliana.gaf; downloaded from Gramene, <https://www.gramene.org>) and applying Fisher's exact test. GO terms were enriched with $P < 0.05$.

Gene expression by reverse transcription-qPCR

Total RNA was reverse transcribed into cDNA using oligo dT primer and diluted cDNA used for qPCR, as described by Ben Abdallah and Bauer (2016). Absolute normalized gene expression values were calculated based on mass standard curve analysis and reference gene normalization (Stephan et al., 2019). Primers for qPCR are listed in Table S1.

Statistical analysis

R was used to perform statistical analyses by one-way analysis of variance (ANOVA) in conjunction with Tukey's honest significant difference (HSD) test ($\alpha = 0.05$). Significant differences with $P < 0.05$ are indicated by different letters.

DATA AVAILABILITY STATEMENT

Biological materials will be available upon request. The transcriptome data set is available for download under GEO number GSE152417.

ACKNOWLEDGEMENTS

We acknowledge the excellent technical assistance of M. Graf, E. Klemp and K. Weber for GC-MS and EA-IRMS measurements. We thank Vera Wewer (University of Cologne) for her advice regarding the establishment of the lipid extraction protocol. The authors thank E. Wieneke for help with gene expression studies. We thank the Genomics and Transcriptomics Laboratory, BMFZ, HHU, for RNA-seq and helpful advice. We are grateful to Maria C. Albani (University of Cologne) for her critical reading of the manuscript. We thank Mary Njeri Ngigi for help in conducting leaf starch quantification assays. This project was funded by the Deutsche Forschungsgemeinschaft (DFG) under Germany's Excellence Strategy (EXC-2048/1, project ID 390686111). The work received funding from the Deutsche Forschungsgemeinschaft international graduate school GRK 2466/1. HL was the recipient of a doctoral fellowship from Northwest A&F University, College of Horticulture, Yangling, China. Open Access funding enabled and organized by ProjektDEAL.

AUTHOR CONTRIBUTIONS

AS, HL, H-JM, TM-A and CK: acquisition of data. AS, HL, H-JM, TM-A, CK, GC and PB: analysis and interpretation of data. AS, TM-A and PB: conception and design. AS and PB: drafting the article. AS, HL, H-JM, TM-A, CK, GC and PB: revising the article.

CONFLICT OF INTEREST

The authors have no conflicts of interest to declare.

SUPPORTING INFORMATION

Additional Supporting Information may be found in the online version of this article.

Figure S1. Experimental outline.

Figure S2. Whole plant morphology.

Figure S3. Additional internode cross-section analysis.

Figure S4. Starch contents in leaves per dry matter.

Figure S5. Analysis of nutrient storage in roots.

Figure S6. Effect of prolonged cytokinin treatment and dissection of the annual zone.

Figure S7. Effect of auxin treatment on cambium activity in the perennial zone.

Figure S8. Effect of gibberellic acid treatment on cambium activity in the perennial zone.

Figure S9. Effect of ethylene on cambium activity in the perennial zone.

Figure S10. Hierarchical clustering and principal component analysis of RNA-sequencing data.

Table S1. Reverse transcription qPCR primers

Table S2. Spreadsheet with RNA-sequencing (RNA-seq) gene expression data set.

Table S3. Enriched GO terms in the comparison of stage I_PZ and stage II_PZ.

Table S4. Enriched GO terms in the comparison of stage I_PZ and stage III_PZ.

Table S5. Enriched GO terms in the comparison of stage I_PZ and stage IV_PZ.

Table S6. Enriched GO terms in the comparison of stage I_PZ and stage IV_AZ_si.

Table S7. Enriched GO terms in the comparison of stage I_PZ and stage IV_AZ_if.

Table S8. Enriched GO terms in the comparison of stage II_PZ and stage III_PZ.

Table S9. Enriched GO terms in the comparison of stage II_PZ and stage IV_PZ.

Table S10. Enriched GO terms in the comparison of stage II_PZ and stage IV_AZ_si.

Table S11. Enriched GO terms in the comparison of stage II_PZ and stage IV_AZ_if.

Table S12. Enriched GO terms in the comparison of stage III_PZ and stage IV_PZ.

Table S13. Enriched GO terms in the comparison of stage III_PZ and stage IV_AZ_si.

Table S14. Enriched GO terms in the comparison of stage III_PZ and stage IV_AZ_if.

Table S15. Enriched GO terms in the comparison of stage IV_PZ and stage IV_AZ_si.

Table S16. Enriched GO terms in the comparison of stage IV_PZ and stage IV_AZ_if.

Table S17. Enriched GO terms in the comparison of stage IV_AZ_si and stage IV_AZ_if.

Table S18. Enriched GO terms in the comparison all PZ stages (stages I, II, III, and IV_PZ) and all AZ stages (stages IV_AZ_si, _if).

Table S19. Gene expression data of cytokinin signaling, biosynthesis and catabolism genes.

REFERENCES

- Agusti, J., Lichtenberger, R., Schwarz, M., Nehlin, L. and Greb, T. (2011) Characterization of transcriptome remodeling during cambium formation identifies MOL1 and RUL1 as opposing regulators of secondary growth. *PLoS Genet*, **7**, e1001312.
- Alexa, A. and Rahnenfuhrer, J. (2010) topGO: enrichment analysis for gene ontology. R package version 2
- Altschul, S.F., Gish, W., Miller, W., Myers, E.W. and Lipman, D.J. (1990) Basic local alignment search tool. *J. Mol. Biol.* **215**, 403–410.
- Anders, S., Pyl, P.T. and Huber, W. (2015) HTSeq—a Python framework to work with high-throughput sequencing data. *Bioinformatics*, **31**, 166–169.
- Andrews, S. (2010) FastQC: a quality control tool for high throughput sequence data (<https://www.bioinformatics.babraham.ac.uk/projects/fastqc/>)
- Ben Abdallah, H. and Bauer, P. (2016) Quantitative Reverse Transcription-qPCR-based gene expression analysis in plants. In *Plant Signal Transduction. Methods in Molecular Biology 1363*. (Botella, J. and Botella, M., eds). New York, NY: Humana Press.
- Bergonzi, S. and Albani, M.C. (2011) Reproductive competence from an annual and a perennial perspective. *J. Exp. Bot.* **62**, 4415–4422.
- Bergonzi, S., Albani, M.C., van Themaat, E.V.L., Nordström, K.J., Wang, R., Schneeberger, K., Moerland, P.D. and Coupland, G. (2013) Mechanisms of age-dependent response to winter temperature in perennial flowering of *Arabis alpina*. *Science*, **340**, 1094–1097.
- Bolger, A.M., Lohse, M. and Usadel, B. (2014) Trimmomatic: a flexible trimmer for Illumina sequence data. *Bioinformatics*, **30**, 2114–2120.
- Bray, N.L., Pimentel, H., Melsted, P. and Pachter, L. (2016) Near-optimal probabilistic RNA-seq quantification. *Nat. Biotechnol.* **34**, 525–527.
- Denis, E., Kbir, N., Mary, V., Claisse, G., Conde, E.S.N., Kreis, M. and Deveaux, Y. (2017) WOX14 promotes bioactive gibberellin synthesis and vascular cell differentiation in *Arabidopsis*. *Plant J.* **90**, 560–572.
- Doolittle, R.F. (1986) Of URFs and ORFs: A primer on how to analyze derived amino acid sequences. University Science Books.
- Eviatar-Ribak, T., Shalit-Kaneh, A., Chappell-Maor, L., Amsellem, Z., Eshed, Y. and Lifschitz, E. (2013) A cytokinin-activating enzyme promotes tuber formation in tomato. *Curr. Biol.* **23**, 1057–1064.
- Fischer, U., Kucukoglu, M., Helariutta, Y. and Bhalerao, R.P. (2019) The dynamics of cambial stem cell activity. *Annu. Rev. Plant Biol.* **70**, 293–319.
- Furze, M.E., Trumbore, S. and Hartmann, H. (2018) Detours on the phloem sugar highway: stem carbon storage and remobilization. *Curr. Opin. Plant Biol.* **43**, 89–95.
- Grillo, M.A., Li, C., Fowlkes, A.M., Briggeman, T.M., Zhou, A., Schemske, D.W. and Sang, T. (2009) Genetic architecture for the adaptive origin of annual wild rice, *Oryza nivara*. *Evolution*, **63**, 870–883.
- Guo, C., Xu, Y., Shi, M., Lai, Y., Wu, X., Wang, H., Zhu, Z., Poethig, R.S. and Wu, G. (2017) Repression of miR156 by miR159 regulates the timing of the juvenile-to-adult transition in *Arabidopsis*. *Plant Cell*, **29**, 1293–1304.
- Hajra, A.K. (1974) On extraction of acyl and alkyl dihydroxyacetone phosphate from incubation mixtures. *Lipids*, **9**, 502–505.
- Hartmann, A., Senning, M., Hedden, P., Sonnewald, U. and Sonnewald, S. (2011) Reactivation of meristem activity and sprout growth in potato tubers require both cytokinin and gibberellin. *Plant Physiol.* **155**, 776–796.
- Heidel, A.J., Kiefer, C., Coupland, G. and Rose, L.E. (2016) Pinpointing genes underlying annual/perennial transitions with comparative genomics. *BMC Genom.* **17**, 921.
- Hu, F.Y., Tao, D.Y., Sacks, E. et al. (2003) Convergent evolution of perenniality in rice and sorghum. *Proc. Natl. Acad. Sci. U S A*, **100**, 4050–4054.
- Hughes, P.W., Soppe, W.J.J. and Albani, M.C. (2019) Seed traits are pleiotropically regulated by the flowering time gene PERPETUAL FLOWERING 1 (PEP1) in the perennial *Arabis alpina*. *Mol. Ecol.* **28**, 1183–1201.
- Hyun, Y., Richter, R. and Coupland, G. (2017) Competence to flower: age-controlled sensitivity to environmental cues. *Plant Physiol.* **173**, 36–46.
- Hyun, Y., Vincent, C., Tilmes, V., Bergonzi, S., Kiefer, C., Richter, R., Martinez-Gallegos, R., Severing, E. and Coupland, G. (2019) A regulatory circuit conferring varied flowering response to cold in annual and perennial plants. *Science*, **363**, 409–412.
- Immanen, J., Nieminen, K., Smolander, O.P. et al. (2016) Cytokinin and auxin display distinct but interconnected distribution and signaling profiles to stimulate cambial activity. *Curr. Biol.* **26**, 1990–1997.
- Karl, R. and Koch, M.A. (2013) A world-wide perspective on crucifer speciation and evolution: phylogenetics, biogeography and trait evolution in tribe Arabideae. *Ann. Bot.* **112**, 983–1001.
- Kiefer, C., Severing, E., Karl, R., Bergonzi, S., Koch, M., Tresch, A. and Coupland, G. (2017) Divergence of annual and perennial species in the Brassicaceae and the contribution of cis-acting variation at FLC orthologues. *Mol. Ecol.* **26**, 3437–3457.

- Kim, D.H., Doyle, M.R., Sung, S. and Amasino, R.M. (2009) Vernalization: Winter and the timing of flowering in plants. *Annu. Rev. Cell Dev. Biol.* **25**, 277–299.
- Kim, D., Langmead, B. and Salzberg, S.L. (2015) HISAT: a fast spliced aligner with low memory requirements. *Nat Methods*, **12**, 357–360.
- Kucukoglu, M., Nilsson, J., Zheng, B., Chaaboukimni, S. and Nilsson, O. (2017) WUSCHEL-RELATED HOMEBOX4 (WOX4)-like genes regulate cambial cell division activity and secondary growth in Populus trees. *New Phytol.* **215**, 642–657.
- Lazaro, A., Obeng-Hinneh, E. and Albani, M.C. (2018) Extended vernalization regulates inflorescence fate in Arabis alpina by stably silencing PERPETUAL FLOWERING1. *Plant Physiol.* **176**, 2819–2833.
- Matsumoto-Kitano, M., Kusumoto, T., Tarkowski, P., Kinoshita-Tsujimura, K., Vaclavikova, K., Miyawaki, K. and Kakimoto, T. (2008) Cytokinins are central regulators of cambial activity. *Proc. Natl. Acad. Sci. U S A*, **105**, 20027–20031.
- McCarthy, D.J., Chen, Y. and Smyth, G.K. (2012) Differential expression analysis of multifactor RNA-Seq experiments with respect to biological variation. *Nucleic Acids Res.* **40**, 4288–4297.
- Netzer, F., Herschbach, C., Oikawa, A., Okazaki, Y., Dubbert, D., Saito, K. and Rennenberg, H. (2018) Seasonal alterations in organic phosphorus metabolism drive the phosphorus economy of annual growth in *F. sylvatica* trees on P-impooverished soil. *Front Plant Sci.* **9**, 723.
- Nieminen, K., Immanen, J., Laxell, M. et al. (2008) Cytokinin signaling regulates cambial development in poplar. *Proc. Natl. Acad. Sci. U S A*, **105**, 20032–20037.
- Park, J.Y., Kim, H. and Lee, I. (2017) Comparative analysis of molecular and physiological traits between perennial Arabis alpina Pajares and annual Arabidopsis thaliana Sy-0. *Sci. Rep.* **7**, 13348.
- Robinson, M.D., McCarthy, D.J. and Smyth, G.K. (2010) edgeR: a Bioconductor package for differential expression analysis of digital gene expression data. *Bioinformatics*, **26**, 139–140.
- Sauter, J.J. and van Cleve, B. (1994) Storage, mobilization and interrelations of starch, sugars, protein and fat in the ray storage tissue of poplar trees. *Trees*, **8**, 297–304.
- Sauter, J.J. and Wellenkamp, S. (1998) Seasonal changes in content of starch, protein and sugars in the twig wood of *Salix caprea* L. *Holzforchung-International Journal of the Biology, Chemistry, Physics and Technology of Wood*, **52**, 255–262.
- Sergeeva, A., Mettler-Altmann, T., Liu, H., Mai, H.-J. and Bauer, P. (2021) Glycerolipid profile differences between perennial and annual stem zones in the perennial model plant *Arabis alpina*. *Plant Direct*. In press
- Smith, A.M. and Zeeman, S.C. (2006) Quantification of starch in plant tissues. *Nat. Protoc.* **1**, 1342–1345.
- Stephan, L., Tilmes, V. and Hülskamp, M. (2019) Selection and validation of reference genes for quantitative Real-Time PCR in Arabis alpina. *PLoS One*, **14**, e0211172.
- Suer, S., Agusti, J., Sanchez, P., Schwarz, M. and Greb, T. (2011) WOX4 imparts auxin responsiveness to cambium cells in Arabidopsis. *Plant Cell*, **23**, 3247–3259.
- Thomas, H. (2013) Senescence, ageing and death of the whole plant. *New Phytol.* **197**, 696–711.
- Vayssières, A., Mishra, P., Roggen, A., Neumann, U., Ljung, K. and Albani, M.C. (2020) Vernalization shapes shoot architecture and ensures the maintenance of dormant buds in the perennial Arabis alpina. *New Phytol.*
- Wang, R., Farrona, S., Vincent, C., Joecker, A., Schoof, H., Turck, F., Alonso-Blanco, C., Coupland, G. and Albani, M.C. (2009) PEP1 regulates perennial flowering in Arabis alpina. *Nature*, **459**, 423–427.
- Watanabe, M., Netzer, F., Tohge, T., Orf, I., Brotman, Y., Dubbert, D., Fernie, A.R., Rennenberg, H., Hoefgen, R. and Herschbach, C. (2018) Metabolome and lipidome profiles of Populus x canescens twig tissues during annual growth show phospholipid-linked storage and mobilization of C, N, and S. *Front Plant Sci.* **9**, 1292.
- Wewer, V., Dombink, I., vom Dorp, K. and Dörmann, P. (2011) Quantification of sterol lipids in plants by quadrupole time-of-flight mass spectrometry. *J Lipid Res.* **52**, 1039–1054.
- Zhang, L. and Guo, C. (2020) The important function of Mediator complex in controlling the developmental transitions in plants. *Int J Mol Sci.* **21**, E2733.